10th World Congress on Structural and Multidisciplinary Optimization
May 19 - 24, 2013, Florida, USA

Level Set-based Topology Optimization of Acoustic Metamaterials

Masaki Otomori[1], Lirong Lu[2], Shinji Nishiwaki[3], Takayuki Yamada[4], Kazuhiro Izui[5], Takashi Yamamoto[6]

[1] Kyoto University, Kyoto, Japan, otomori.masaki@gmail.com
[2] Kyoto University, Kyoto, Japan, lirong.lu@ks4.ecs.kyoto-u.ac.jp
[3] Kyoto University, Kyoto, Japan, shinji@prec.kyoto-u.ac.jp
[4] Kyoto University, Kyoto, Japan, takayuki@me.kyoto-u.ac.jp
[5] Kyoto University, Kyoto, Japan, izui@me.kyoto-u.ac.jp
[6] Kogakuin University, Tokyo, Japan, takashi_yamamoto@cc.kogakuin.ac.jp

1. Abstract
This paper discusses a topology optimization method for the design of acoustic metamaterials that exhibit negative bulk modulus, using level set-based boundary expression. The purpose of the optimization problem here is to find optimal configurations of acoustic metamaterial unit cells composed of rubber and epoxy that achieve a negative effective bulk modulus. The presence of grayscale areas in an optimal configuration significantly affects the performance of acoustic metamaterials, therefore, in this study, we use a level set-based approach to avoid this problem. The effective bulk modulus of the acoustic metamaterials is computed based on reflection and transmission coefficients. The optimization problem is formulated to minimize the effective bulk modulus at a target frequency. The optimization algorithm uses the adjoint variable method (AVM) to obtain design sensitivities and the finite element method (FEM) to solve the acoustic wave propagation problem, the adjoint problem, and the reaction diffusion equation used to update the level set function. Finally, several numerical examples including two- and three-dimensional problems are provided to confirm the utility and validity of the proposed method.

2. Keywords: Topology optimization, Level set method, Acoustic metamaterials, Negative bulk modulus, Adjoint variable method

3. Introduction
Acoustic metamaterials are artificially engineered materials that are designed to have extraordinary acoustic properties, such as a negative effective bulk modulus and negative effective mass density. Several novel applications using such acoustic metamaterials have been proposed, such as sound isolation devices, acoustic cloaking [1], acoustic super lenses [2], and others. Most metamaterials consist of periodic structures of unit cells that are sufficiently small compared to the wavelength of a target frequency. While the constituent materials themselves do not exhibit extraordinary properties, the overall array of periodic structures can be considered as an effectively homogeneous acoustic material, and such materials exhibit extraordinary properties globally, such as negative effective properties. For the design of acoustic metamaterials, Liu et al. [3] first experimentally demonstrated that composite materials composed of lead balls coated with silicone rubber and epoxy resin show a negative bulk modulus. Subsequently, considerable research exploring acoustic metamaterials that exhibit negative bulk modulus and negative mass density have been reported. However, the performance of such acoustic metamaterials is very sensitive to their unit cell design and it is usually difficult or excessively time-consuming to find appropriate unit cell designs that exhibit desirable properties using trial and error methods. Therefore there is a need for a systematic design approach, such as topology optimization, that facilitates obtaining desirable unit cell designs.

This paper presents a level set-based topology optimization method for the design of negative bulk modulus acoustic metamaterials. The purpose of the optimization problem here is to find optimized configurations of acoustic metamaterials composed of rubber and epoxy that achieve a negative effective bulk modulus at a prescribed frequency. In this study, we applied a level set-based topology optimization method [4] to avoid the inclusion of grayscale areas in the configurations obtained by the optimization. To compute the effective bulk modulus of the acoustic metamaterials, we retrieve the effective acoustic properties, based on the values of reflected and transmitted sound powers, using a computational method [5] that is an extension of the method originally proposed to compute the effective properties of electro-

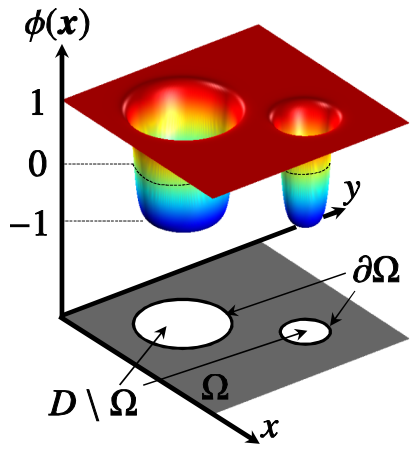

Figure 1: Fixed design domain D and level set function ϕ

magnetic metamaterials based on S parameters [6]. The optimization problem is formulated to minimize the effective bulk modulus to obtain acoustic metamaterial designs that exhibit a negative bulk modulus. The optimization algorithm uses the adjoint variable method (AVM) for sensitivity analysis and the finite element method (FEM) for solving the acoustic wave propagation problem, the adjoint problem, and the reaction diffusion equation used to update the level set function. Several numerical examples for two- and three- dimensional effective bulk modulus minimization problems are provided to confirm the utility and validity of the proposed method. The optimization results show that the obtained configurations behave as structures having negative bulk modulus at the prescribed operating frequency.

4. Formulation

4.1. Level Set-Based Topology Optimization

We briefly explain the level set-based topology optimization method applied in this study. In a level set-based topology optimization, as shown in Fig.1, the material domain Ω, structural boundaries $\partial\Omega$, and $D \setminus \Omega$ are implicitly expressed as follows:

$$\begin{cases} 0 < \phi(\boldsymbol{x}) \leqslant 1 & \text{if } \forall \boldsymbol{x} \in \Omega \backslash \partial\Omega \\ \phi(\boldsymbol{x}) = 0 & \text{if } \forall \boldsymbol{x} \in \partial\Omega \\ -1 \leqslant \phi(\boldsymbol{x}) < 0 & \text{if } \forall \boldsymbol{x} \in D \backslash \Omega. \end{cases} \tag{1}$$

Next, using above expressions, the optimization problem can be formulated as

$$\begin{aligned} \inf_{\phi} \quad & F(\chi_\Omega(\phi)) = \int_D f(\boldsymbol{x}) \chi_\Omega(\phi) \mathrm{d}\Omega \\ \text{subject to} \quad & G(\chi_\Omega(\phi)) = \int_D \chi_\Omega(\phi) \mathrm{d}\Omega - V_{\max} \leqslant 0, \end{aligned} \tag{2}$$

where F and G are the objective and constraint functionals, respectively, and $V_{\max}$ is the upper limit value of the constraint functional. $\chi_\Omega(\phi)$ is the characteristic function defined as

$$\chi_\Omega(\phi) = \begin{cases} 1 & \text{if } \phi \geqslant 0 \\ 0 & \text{if } \phi < 0. \end{cases} \tag{3}$$

The level set function $\phi(\boldsymbol{x})$ in the optimization problem defined above can be discontinuous everywhere in fixed design domain D, so regularization is required. Here, the optimization problem is regularized using a Tikhonov regularization method in which the regularization term $R = \int_D \frac{1}{2}\tau |\nabla\phi(\boldsymbol{x})|^2 \mathrm{d}\Omega$ is added to the primary objective functional, as follows.

$$\begin{aligned} \inf_{\phi} \quad & F_R(\chi_\Omega, \phi) = F + R \\ \text{subject to} \quad & G(\chi_\Omega) \leqslant 0, \end{aligned} \tag{4}$$

where τ is a regularization parameter. Next, the optimization problem is replaced by a problem with no constraint functionals, using the Lagrange method for undetermined multipliers, as follows.

$$\inf_{\phi} \quad \bar{F}_R(\chi_\Omega, \phi) = F_R + \lambda G, \tag{5}$$

where $\bar{F_R}$ and λ are the Lagrangian and the Lagrange multiplier, respecitvely.

Here, to obtain a level set function that represents an optimal configuration, we introduce a fictitious time t and derive the following time evolutionary equation, assuming that the time variation of the level set function is proportional to the gradient of the Lagrangian $\bar{F_R}$, as follows.

$$\frac{\partial \phi}{\partial t} = -K(\phi)\bar{F}'_R, \tag{6}$$

where $K(\phi) > 0$ is a coefficient of proportionality. The following reaction diffusion equation is obtained by substituting Eq.(5) into Eq.(6) and imposing a Dirichlet boundary condition on the non-design boundary, and a Neumann boundary condition on the other boundaries, to represent the level set function independently of the exterior of the fixed design domain.

$$\begin{cases} \dfrac{\partial \phi}{\partial t} = -K(\phi)\Big(\bar{F}' - \tau\nabla^2\phi\Big) & \\ \dfrac{\partial \phi}{\partial n} = 0 & \text{on} \quad \partial D \setminus \partial D_N \\ \phi = 1 & \text{on} \quad \partial D_N, \end{cases} \tag{7}$$

where $\bar{F} = F + \lambda G$. The optimization problem is now replaced by a problem to solve the above reaction diffusion equation, whose solutions are candidate optimal solutions.

4.2. Effective bulk modulus

Fokin et al.[5] proposed a method for computing the effective acoustic impedance and refractive index of acoustic metamaterials, based on a formulation proposed by Smith et al. [6] used to compute the effective properties of electromagnetic metamaterials. Here, we extend Fokin et al.'s [5] method based on a later Smith et al.'s method [7] so that the formulation becomes symmetric with respect to reflection coefficients R_1 and R_2, which ensures that symmetric optimized configurations are obtained. The effective bulk modulus is computed as follows, based on the reflection and transmission coefficients.

$$K_{\text{eff}} = \frac{K_0}{c\rho_0}\frac{Z}{n}\ , \tag{8}$$

where K_0, ρ_0, c are the bulk modulus, mass density, and speed of sound in a vacuum. Z is the acoustic impedance and n is the index of refraction, given as follows.

$$Z = \sqrt{\frac{(1+R_1)(1+R_2) - T_{21}^2}{(1-R_1)(1-R_2) - T_{21}^2}} \tag{9}$$

$$n = \cos^{-1}\left(\frac{\beta}{2T_{21}}\right)\frac{\lambda}{2\pi d}\ , \tag{10}$$

where β is defined as follows:

$$\beta = 1 - R_1R_2 + T_{21}^2\ , \tag{11}$$

and where R_1, T_{21}, and R_2 are obtained so that

$$R_1 = \frac{\int_{\Gamma_1}(p_1 - p_1^i)p_1^i d\Gamma}{\int_{\Gamma_1} p_1^i p_1^i d\Gamma} \tag{12}$$

$$T_{21} = \frac{\int_{\Gamma_2} p_1 p_1^i d\Gamma}{\int_{\Gamma_2} p_1^i p_1^i d\Gamma} \tag{13}$$

$$R_2 = \frac{\int_{\Gamma_2}(p_2 - p_2^i)p_2^i d\Gamma}{\int_{\Gamma_2} p_2^i p_2^i d\Gamma}. \tag{14}$$

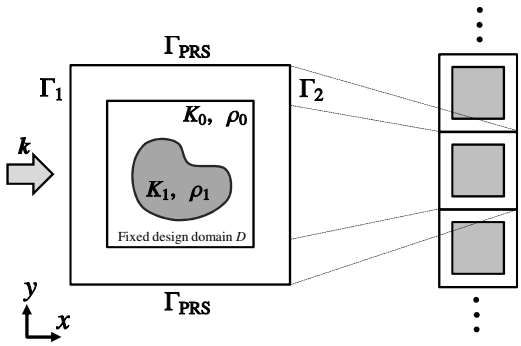

Figure 2: Analysis domain and boundary conditions for two-dimensional problem.

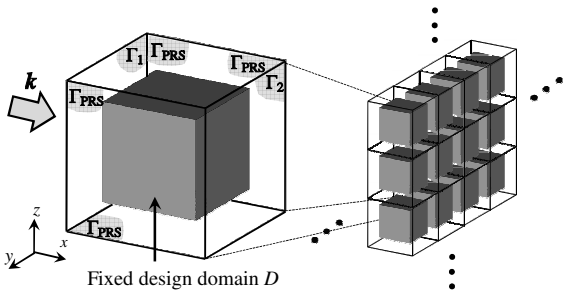

Figure 3: Analysis domain and boundary conditions for three-dimensional problem.

In addition, p_1 and R_1 are the sound pressure and reflection coefficient when an incident sound wave p_1^i enters at boundary Γ_1, respectively, and p_2 and R_2 are the sound pressure and reflection coefficient when an incident sound wave p_2^i enters boundary Γ_2, respectively. T_{21} represents the transmission coefficient from boundary Γ_1 to Γ_2 when an incident sound wave p_1^i enters at boundary Γ_1.

4.3. Acoustic wave propagation problem

In the acoustic metamaterial design problem, the acoustic wave propagation problem for the metamaterial unit cell is solved and the effective acoustic properties, the effective bulk modulus and the effective mass density, are obtained. Figure 2 shows the fixed design domain and boundary conditions for the two-dimensional problem. An incident wave enters the domain from the left and the upper and lower boundaries are set as perfectly reflecting surfaces, represented as Γ_{PRS}. Figure 3 shows the fixed design domain and boundary conditions for the three-dimensional problem. In addition to the upper and lower boundaries, the front and rear boundaries are also set as perfectly reflecting surfaces, Γ_{PRS}. The governing equation is given by the Helmholtz equation, as follows, using sound pressure p_1, mass density ρ, and bulk moduls K of the constituent material.

$$\nabla \cdot \left(\rho^{-1} \nabla p_1\right) + \omega^2 K^{-1} p_1 = 0, \tag{15}$$

where ω represents the angular frequency and k_0 represents the wave number in a vacuum, defined as $k_0 = \omega\sqrt{\rho_0/K_0}$.

The boundary conditions are given as follows.

$$\boldsymbol{n} \cdot \left(\rho^{-1} \nabla p_1\right) + jk_0 p_1 = 2jk_0 p_1^i \qquad \text{on} \quad \Gamma_1 \tag{16}$$

$$\boldsymbol{n} \cdot \left(\rho^{-1} \nabla p_1\right) + jk_0 p_1 = 0 \qquad \text{on} \quad \Gamma_2 \tag{17}$$

$$\boldsymbol{n} \cdot \left(\rho^{-1} \nabla p_1\right) = 0 \qquad \text{on} \quad \Gamma_{\mathrm{PRS}} \tag{18}$$

where $\boldsymbol{n}$ is the normal vector. Sound pressure p_2^i can also be obtained by solving the Helmholtz equation with the location of the input and output boundaries switch, so that boundary condition Eq.(16) applies to Γ_2 and Eq.(17) applies to Γ_1.

4.4. Optimization problem

The purpose of the optimization here is to minimize the real part of the effective bulk modulus at a desired frequency. A typical effective bulk modulus curve is shown in Fig. 4(a), where K' and K'' represent plots of the real and imaginary part of the effective bulk modulus, respectively. The real part of the effective bulk modulus has a positive peak, and a negative peak, where the effective bulk modulus has a desirable negative value. However, if the positive peak lies between the negative peak and the target frequency, that is, if the target frequency is located in the hatched area for the case shown in Fig.4(a), configurations that demonstrate negative effective bulk modulus cannot be obtained directly. For example, if the target frequency is set as shown in Fig.4(b), and the real part of the effective bulk modulus is minimized directly, an increase in the frequency of the resonance frequency results in a decrease of the objective values.

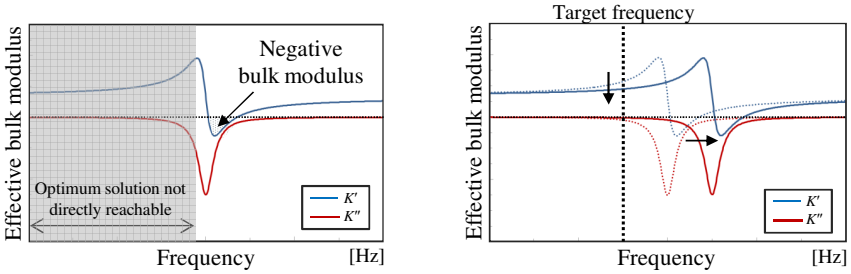

Figure 4: Typical effective bulk modulus curve

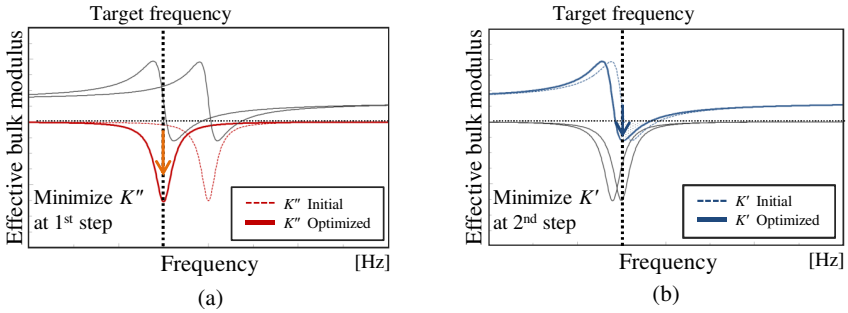

Figure 5: Two-step approach

Thus, in this study, we use a two-step approach in which the imaginary part of bulk modulus K'' is minimized in the first step, as shown in Fig.5(a), and the real part of bulk modulus K' is then minimized in the second step, as shown in Fig.5(b), using the optimal configuration in the first step as the initial configuration. The optimization problem for the first step is described below.

$$\begin{aligned}
&\inf_{\phi} && F = K''_{\text{eff}} && (19)\\
&\text{subject to} && G \leqslant 0 && (20)\\
& && a_1(\chi_\Omega, p_1, \tilde{p_1}) + a_2(p_1, \tilde{p_1}) = l_{p_1}(\tilde{p_1}) \quad \text{for} \quad p_1 \in U, \quad {}^\forall\tilde{p_1} \in U && (21)\\
& && a_1(\chi_\Omega, p_2, \tilde{p_2}) + a_2(p_2, \tilde{p_2}) = l_{p_2}(\tilde{p_2}) \quad \text{for} \quad p_2 \in U, \quad {}^\forall\tilde{p_2} \in U && (22)
\end{aligned}$$

where

$$a_1(\chi_\Omega, p, \tilde{p}) = \int_D \rho^{-1}(\chi_\Omega)\nabla p \cdot \nabla\tilde{p}\mathrm{d}\Omega - \omega^2 \int_D K^{-1}(\chi_\Omega) p\tilde{p}\mathrm{d}\Omega \tag{23}$$

$$a_2(p, \tilde{p}) = jk_0 \int_{\Gamma_1 \cup \Gamma_2} \rho^{-1} p\tilde{p}\mathrm{d}\Gamma \tag{24}$$

$$l_{p_i}(\tilde{p}) = 2jk_0 \int_{\Gamma_i} p^i \tilde{p}\mathrm{d}\Gamma \tag{25}$$

$$U = \{\tilde{p} \in H^1(D)\} \tag{26}$$

The optimization problem for second step is described below.

$$\begin{aligned}
&\inf_{\phi} && F = K'_{\text{eff}} && (27)\\
&\text{subject to} && G \leqslant 0 && (28)\\
& && a_1(\chi_\Omega, p_1, \tilde{p_1}) + a_2(p_1, \tilde{p_1}) = l_{p_1}(\tilde{p_1}) \quad \text{for} \quad p_1 \in U, \quad {}^\forall\tilde{p_1} \in U && (29)\\
& && a_1(\chi_\Omega, p_2, \tilde{p_2}) + a_2(p_2, \tilde{p_2}) = l_{p_2}(\tilde{p_2}) \quad \text{for} \quad p_2 \in U, \quad {}^\forall\tilde{p_2} \in U && (30)
\end{aligned}$$

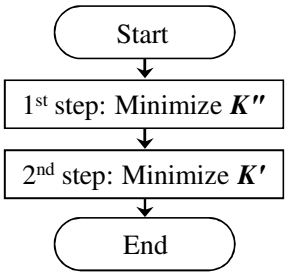

Figure 6: Two-step approach

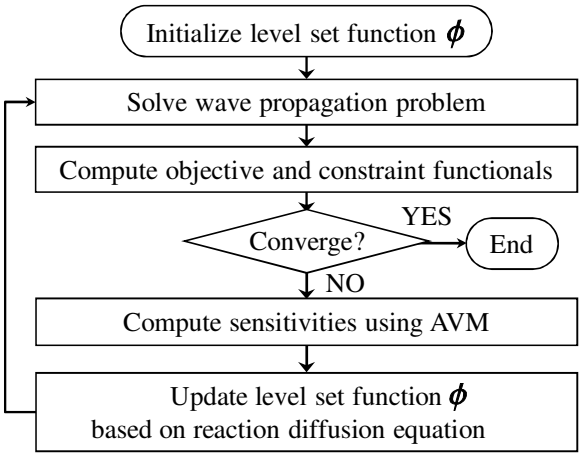

Figure 7: Flowchart of each step

5. Implementation

5.1. Design variable

The material distribution inside the fixed design domain is expressed using the level set function. In our method, we use a reciprocal formulation of the mass density ρ and bulk modulus K, so these are defined using the characteristic function χ_Ω as follows.

$$\rho^{-1} = \left(\rho_1^{-1} - \rho_0^{-1}\right) H(\phi) + \rho_0^{-1} \tag{31}$$

$$K^{-1} = \left(K_1^{-1} - K_0^{-1}\right) H(\phi) + K_0^{-1}, \tag{32}$$

where ρ_1 and K_1 are respectively the mass density and bulk modulus of the solid material, and ρ_0 and K_0 are respectively the mass density and bulk modulus of the background material. $H(\phi)$ is a Heaviside function, approximated as follows in the numerical implementation.

$$H(\phi) = \begin{cases} 0 & (\phi < -w) \\ \frac{1}{2} + \frac{\phi}{w}\left(\frac{15}{16} - \frac{\phi^2}{w^2}\left(\frac{5}{8} - \frac{3}{16}\frac{\phi^2}{w^2}\right)\right) & (-w \leqslant \phi < w) \\ 1 & (w \leqslant \phi), \end{cases} \tag{33}$$

where w is the transition width of the Heaviside function, which is set to a sufficiently small value.

5.2. Optimization algorithm

Figure 6 shows the optimization flowchart. A two-step optimization procedure is used in which the imaginary part of the effective permeability is first minimized and then the real part of the effective permeability is minimized during the second steps.

Figure 7 shows the optimization flowchart for each of the above steps. First, the level set function is initialized. Next, the acoustic wave propagation problem is solved using the Finite Element Method (FEM) and the objective functional and constraint functional are calculated. If the objective functional has converged, the optimization procedure is terminated. If not, the sensitivities of objective and constraint functional are computed using the Adjoint Variable Method (AVM). The level set function is then updated using a reaction diffusion equation and the process returns to the second step.

6. Numerical examples

In this section, we provide several numerical examples for the design of acoustic metamaterials that exhibit negative bulk modulus to confirm the validity of the presented method. For the following examples, we use silicone rubber as the solid material, epoxy as the background material, and air as a constituent in the domain outside the fixed design domain. The bulk modulus of the silicone rubber, epoxy, and air are respectively set as $K_1 = 6.25 \times 10^5(1 + j\eta)$Pa, $K_0 = 5.49 \times 10^9(1 + j\eta)$Pa, and $K_{\text{air}} = 1.47 \times 10^5$Pa. The mass density of the silicone rubber, epoxy, and air are respectively set as $\rho_1 = 1.3 \times 10^3(1 + j\xi)$kg/m^3, $\rho_0 = 1.18 \times 10^3(1 + j\xi)$kg/m^3, and $\rho_{\text{air}} = 1.25$kg/m^3. ξ, η are damping coefficients that are here set so

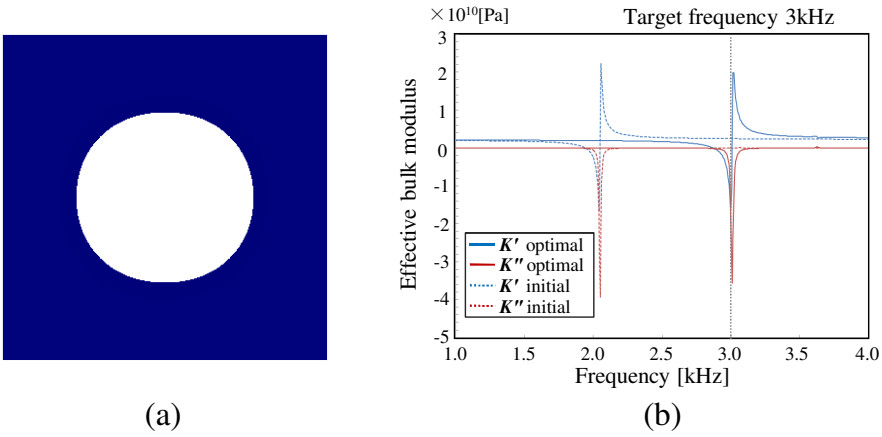

Figure 8: Optimization results of 2-dimensional problem targeting 3000Hz: (a) optimal configuration of silicone rubber(blue) and epoxy(white); (b) effective bulk modulus curve.

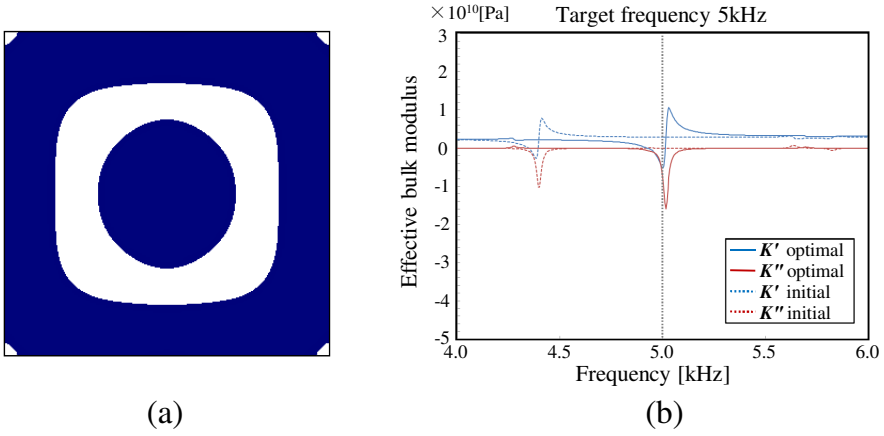

Figure 9: Optimization results of 2-dimensional problem targeting 5000Hz: (a) optimal configuration of silicone rubber(blue) and epoxy(white); (b) effective bulk modulus curve.

that $\xi = -0.003$ and $\eta = 0.003$. A configuration filled with the solid material in the fixed design domain is used as an initial configuration in all the examples.

For the two-dimensional problems, the analysis domain shown in Fig.2 is 12mm×12mm in size and the fixed design domain is 8mm×8mm. The analysis domain is discretized using 120 × 120 square elements. For the three-dimensional problems, the analysis domain shown in Fig.3 is 12mm ×12mm×12mm in extent and the fixed design domain is 8mm×8mm×8mm. The analysis domain is discretized using 48×48×48 cubic elements.

6.1. Two-dimensional problem targeting 3000Hz

We first address a two-dimensional design problem that has a target frequency of 3000Hz. Figure 8 shows the optimal configuration and a graph of the frequency response versus the effective bulk modulus for the initial and optimal configurations. The negative peak of the real part of the effective bulk modulus reached the target frequency. The values of the effective bulk modulus for the initial and optimal configuration at 3000Hz are 2.50×10^9Pa and -1.61×10^{10}Pa, respectively.

6.2. Two-dimensional problem targeting 5000Hz

Next, we consider a two-dimensional design problem with a target frequency of 5000Hz. Figure 9 shows the optimal configuration and a graph of the frequency response versus the effective bulk modulus for the initial and optimal configurations. Again, the negative peak of the real part of the effective bulk modulus

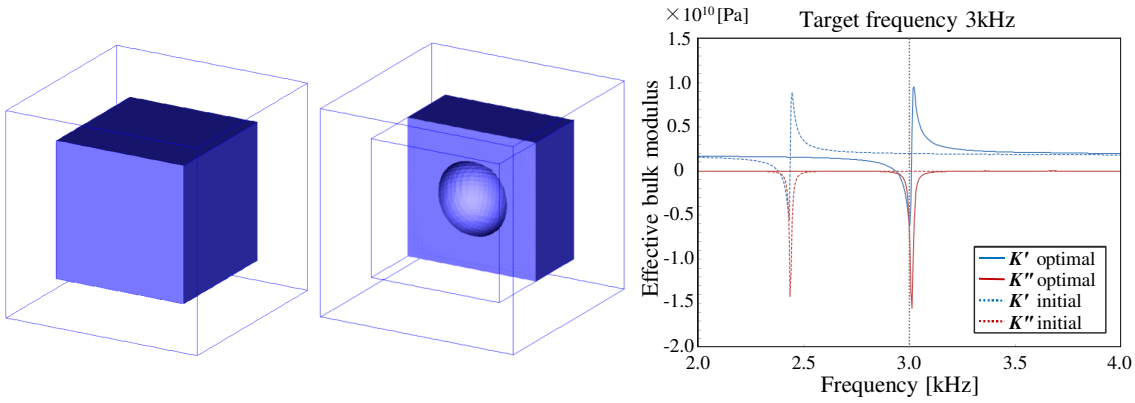

Figure 10: Optimization results of 3-dimensional problem targeting 3000Hz: (a) optimal configuration; (b) its cross-sectional view; (c) effective bulk modulus curve.

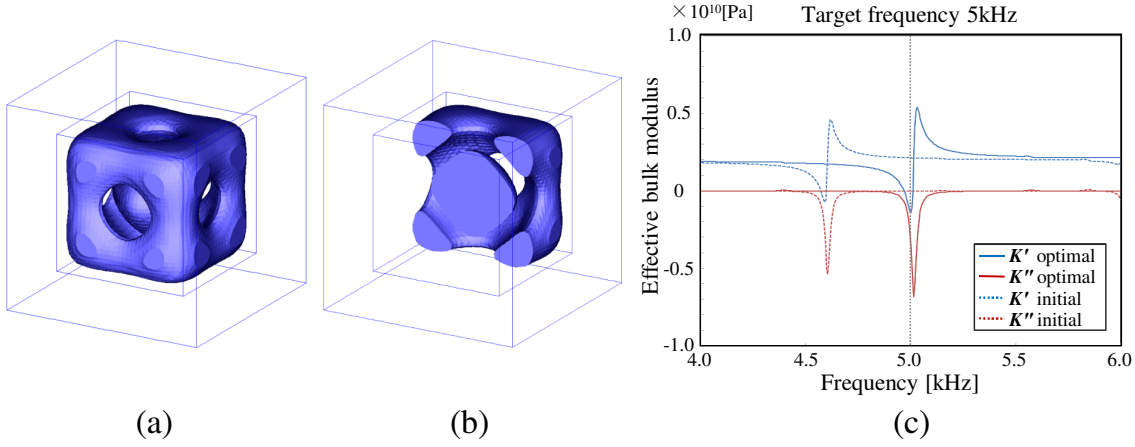

Figure 11: Optimization results of 3-dimensional problem targeting 5000Hz: (a) optimal configuration; (b) its cross-sectional view; (c) effective bulk modulus curve.

reached the target frequency. The effective bulk modulus values at 5000Hz for the initial and optimal configuration were 2.83×10^9Pa and -5.24×10^9Pa, respectively.

6.3. Three-dimensional problem targeting 3000Hz

Here, we address a three-dimensional design problem with a target frequency of 3000Hz. Figure 10(a) and Fig. 10(b) show the optimal configuration and a cross-sectional view of the interior, respectively. Figure 10(c) shows a graph of frequency versus the effective bulk modulus for the initial and optimal configurations. The negative peak of the real part of the effective bulk modulus reached the target frequency. The values of the effective bulk modulus at 3000Hz for the initial and optimal configurations were 1.98×10^9Pa and -6.20×10^9Pa, respectively.

6.4. Three-dimensional problem targeting 5000Hz

Finally, we show a three-dimensional design problem with a target frequency of 5000Hz. Figure 11(a) and Fig. 11(b) show the optimal configuration and a corresponding cross-sectional view, respectively. Figure 11(c) shows a graph of frequency versus the effective bulk modulus for the initial and optimal configurations. Again, the negative peak of the real part of the effective bulk modulus reached the target frequency. The values of the effective bulk modulus at 5000Hz for the initial and optimal configurations were 2.12×10^9Pa and -1.40×10^9Pa, respectively.

7. Conclusion

This paper presented a level set-based topology optimization method for the design of acoustic metamaterials. The effective bulk modulus of the acoustic metamaterials was obtained based on reflection and transmission coefficients. The optimization problem was formulated to minimize the effective bulk modulus at a target frequency. The sensitivity analysis was performed using the Adjoint Variable Method (AVM) and the level set function was updated using a reaction-diffusion equation. The numerical examples demonstrated that the proposed method obtains clear optimal configurations, and that the bulk modulus values are reduced so that they successfully assume negative values at the prescribed target frequencies.

8. References

[**1**] H. Chen, and C. T. Chan, Acoustic cloaking in three dimensions using acoustic metamaterials, *Applied Physics Letters*, 91(18), 183518, 2007.

[**2**] J. Li, L. Fok, X. Yin, G. Bartal and X. Zhang, Experimental demonstration of an acoustic magnifying hyperlens, *Nature Materials*, 8(12), 931-934, 2009.

[**3**] Z. Liu, X. Zhang, Y. Mao, Y. Y. Zhu, Z. Yang, C. T. Chan and P. Sheng, Locally resonant sonic materials, *Science*, 289(5485), 1734-1736, 2000.

[**4**] T. Yamada, K. Izui, S. Nishiwaki and A. Takezawa, A topology optimization method based on the level set method incorporating a fictitious interface energy, *Computer Methods in Applied Mechanics and Engineering*, 199(45-48), 2876-2891, 2010.

[**5**] V. Fokin, M. Ambati, C. Sun and X. Zhang, Method for retrieving effective properties of locally resonant acoustic metamaterials, *Physical Review B*, 76(14), 144302, 2007.

[**6**] D. R. Smith, S. Schultz, P. Markoš and C. M. Soukoulis, Determination of effective permittivity and permeability of metamaterials from reflection and transmission coefficients, *Physical Review B*, 65(19), 195104, 2002.

[**7**] D. R. Smith, D. C. Vier, T. Koschny and C. M. Soukoulis, Electromagnetic parameter retrieval from inhomogeneous metamaterials, *Physical Review E*, 71, 036617, 2005.

[**8**] O. Sigmund, Systematic Design of Metamaterials by Topology Optimization, *IUTAM Symposium on Modelling Nanomaterials and Nanosystems* , R. Pyrz and J. C. Rauhe (Eds.), 13, 151-159, 2009,